

PARTICLE IDENTIFICATION WITH A FINE SAMPLING

IONIZATION LOSS DETECTOR*

T. Ludlam, E.D. Platner, V.A. Polychronakos
Brookhaven National Laboratory
Upton, New York 11973

S.J. Lindenbaum
BNL and City College of CUNY
New York, NY 10031

E. Rosso, P. Queru
CERN
Geneva 23, Switzerland

M.A. Kramer, Y. Teramoto
City College of CUNY
New York, NY 10031

T. Akesson, G. Jarlskog, L. Roennborn
University of Lund
Lund, Sweden

Introduction

In a recent series of tests¹ it has been shown that the sensitivity for charged particle identification via the relativistic rise in ionization loss can be enhanced by using longitudinal drift and fast electronics to effect very small sampling intervals. With the chamber geometry illustrated in Fig. 1a (i.e., operation in the "time expansion" mode) electrons from individual ionizing collisions drift sequentially onto the anode wire with a time structure determined by the drift velocity in the gas. After fast pulse shaping the resultant waveform is digitized with a flash-encoding ADC at a frequency of 100MHz. For the tests described in Ref. 1 the smallest sampling interval was 1/4 mm, and the sensitivity of mass (velocity) discrimination was studied for 1 meter of track length with sampling intervals ranging from 1/4 mm/sample to 16 mm/sample, the upper end of this range being typical of conventional ionization sampling devices.

The results of these initial tests are summarized in Fig. 2 as a function of the sample size. The result achieved with 1 meter of conventional sampling (ISIS-1, Ref. 2) is shown for comparison. For large sample sizes the results are comparable to those of traditional techniques, and a significant improvement is achieved when the sampling frequency is increased by roughly an order of magnitude. These results were gotten with a small test chamber in which meter-long tracks were simulated by piecing together many traversals of a single drift gap. We report here on the status of further studies to see whether this improvement in sensitivity can be duplicated with a chamber of practical dimensions and many readout channels.

Test Configuration

For the present tests we use a multiplane chamber incorporating the geometry illustrated in Fig. 1b. Here the sense planes (anode plus field wires) are located symmetrically between planes of cathode wires with electrons drifting from either side. Each sense plane is instrumented with 10 active anode wires. The wire length is 20 cm and the anode wire diameter is 20 μ m. The chamber has 10 such planes (100 active wires) for a total depth along the beam of 40 cm. The test detector, which was constructed by the CERN EF Division, is shown in Fig. 4.

All tests have been carried out with a gas mixture of 80% argon/20% CO₂. The potentials on the cathode and field wires are adjusted to give a drift electric field of ~ 300 V/cm and an avalanche gain (for full

*Work supported by the U.S. Dept. of Energy.

charge collection) of $\sim 10^4$. The drift field was chosen to give an electron drift velocity of 1 cm/ μ sec, $\sim 1/5$ the saturated velocity in this gas mixture. The volume of uniform field (adequate for longitudinal drift measurements of dE/dx) extends to within ± 3 mm of the sense plane and ± 1 mm of the cathode planes. Hence, in principle, 80% of the track length through a chamber of this geometry is usable for ionization loss measurements.

The readout electronics chain is illustrated in Fig. 4. A low-noise, common-base preamplifier is attached directly to the end of each anode wire, followed by a shaping and filter amplifier which consists of a semi-Gaussian integrator with a pole-zero tail cancellation.³ The pulse width (FWHM) of the response to a single cluster of electrons (x-ray source) was set to be 20 nsec. For these tests the outputs of all preamplifiers in a given plane were summed as input to a single shaping amplifier. The shaped signal was digitized with a 6-bit (64 level) flash encoder operating at 100MHz. The digital output from each channel was buffered in a 6 x 256 bit shift register operating at the same clock speed,⁴ allowing the storage of ~ 2.5 μ sec of drift information in each channel. For the chamber configuration of Fig. 1a, and the chosen drift velocity, the total drift time is 1.8 μ sec and each 10 μ sec digitizing interval corresponds to .27 mm of track length.

The results reported here were obtained in a 3.5 GeV/c positive beam at the CERN Proton Synchrotron. Protons, pions and electrons were tagged with a pair of threshold Cerenkov counters and a lead glass shower counter. The beam was normally incident on the sense wire planes as indicated in Fig. 1.

Test Results

Figure 5 shows the ADC response for a single track crossing a drift cell. The first signal arrival at the anode wire occurs in bin 19, prior to which one sees a DC off-set level of ~ 13 counts which was provided in order to study the baseline behavior as the signal develops. Typical structure is observed, corresponding to the sequential arrival of clusters of drifting electrons. Individual clusters (i.e. the results of single ionizing collisions) are not resolved, but are blurred by the effects of electron diffusion, finite pulse shaping width, and the fact that the observed signal in a given time interval is a superposition of ionization loss from either side of the sense plane. At the beginning of the pulse train the signal is characteristically large, corresponding to the portion of track

($\sim \pm 3$ mm) which lies in the high-field region near the sense wire plane. There the drift velocity is essentially saturated, and the collected charge per unit time is greater than that from the uniform drift region by a factor of about 5. For the illustrated track this initial pulse exceeds the dynamic range of the ADC.

Our procedure for evaluating the effectiveness of very fine sampling intervals for particle discrimination is to divide each track into sampling intervals of 2, 4, 16 or 64 of the rudimentary time bins. The charge is integrated in each interval, after subtracting the baseline, and the resultant samples used to evaluate a parametric estimator (e.g. the truncated mean) of the ionization loss for the track. By spreading the ionization charge over many measurements, each involving a small signal, the longitudinal drift technique is extremely sensitive to the stability of the baseline, and changes in the zero level during the charge collection time must be corrected for. Ideally, the signal processing electronics should obviate the need for such corrections. The tail-cancelling networks, for instance, are designed to remove one source of baseline shift. For the circuitry which we used in these tests another source, with similar effect, comes into play for collection times which are long compared to the single-electron shaping time: the cumulative effect of AC coupling in the system gave a time constant of ~ 10 μ sec, which is appreciable compared to the total drift time of ~ 2 μ sec. Hence the level of the baseline falls off during the course of the pulse train at a rate which is proportional to the signal charge. To the extent that the ADC data include a complete time history of the signal on the wire, this effect can be corrected for, on a track-by-track basis as illustrated in Fig. 5. Figure 6 shows the signal, for incident protons, averaged over many track segments. The shaded area indicates the contribution accounted for by the baseline correction, which is substantial. We stress that this off-line correction, which is necessary for the analysis of the present data, should not be necessary in principle and indeed is not consistent with the requirements of a practical detector. We are presently designing circuits which will incorporate dynamic baseline restoration in an effectively DC coupled amplifier chain.

In Fig. 7 we show pulse height distributions obtained from the data for electron and proton tracks, for both "large" and "small" sampling intervals. The 17 mm samples (Fig. 7a) were obtained by summing the digitized information over groups of 64 successive 10 nsec time bins. The 1/2 mm samples are similarly obtained, by summing in groups of 2. (Two successive digitizings span a time interval equal to the 20 nsec width of the shaping circuit's response to an impulse of charge.) The horizontal scales are in ADC counts, with 2 ADC counts corresponding roughly to the signal charge induced by a single drifting electron. The distributions in Fig. 7a are consistent with results obtained from conventional measurements of ionization loss in similar thicknesses of gas, except that the delta ray tail at large pulse heights is somewhat suppressed in our data by the limited dynamic range of the flash encoders. The small samples (Fig. 7b) exhibit a more pronounced dependence of the shape of the energy loss distribution on particle velocity: both the protons (minimum ionizing) and the electrons (on the Fermi plateau) have some contribution at zero pulse height, the electrons having a substantially broader spectrum. The relativistic rise, as measured, e.g. by the ratio of most probable energy loss for electrons and protons, is larger for the smaller sample size.

To compare the sensitivity for particle identification with previous results, we calculate the truncated mean pulse height for 1-meter track lengths. At the time of this test only 6 of the 10 planes in our chamber were fully instrumented with readout electronics, corresponding to ~ 20 cm of usable track length for

each incident particle. The useful track length was further restricted, by about a factor of two, by the requirement that the initial pulse from charge near the anode wire not exceed the range of the ADC. This was necessary for the baseline reconstruction discussed above. Hence, although one of the aims of this test was to investigate the performance of a device incorporating many of the characteristics of a full-scale detector, it was still necessary to assemble 1-meter track lengths from data accumulated over several successive particle traversals.

Having assembled an ensemble of 1-meter track lengths, each track was subdivided into various sampling intervals ranging from small (~ 2000 samples/meter) to large (~ 60 samples/meter) and the truncated mean, retaining the 40% smallest pulse heights, was calculated for each case. The results as a function of sample size, are shown in Fig. 8. The resolving power for distinguishing electrons and protons clearly improves as the sampling frequency is increased. The separation ($S_{ep} = 3.6$) obtained with 17 mm sample size is comparable to that achieved with conventional dE/dx measurements over 1 meter of track length, as indicated by the point labeled ISIS-I on Fig. 2. The same set of tracks shows significantly better separation as the fine-sampling information is exploited. With the smallest sample size (1850 samples/meter of track) the figure of merit S_{ep} is improved by a factor of ~ 2 over the conventional sampling geometry. The origin of this improved sensitivity is made visually clear in Fig. 8 (and is explored in detail in Ref. 1): the relativistic rise is enhanced at small sample sizes, with no degradation in rms width of the truncated mean distributions.

The values of S_{ep} obtained in this test fall systematically below those of our previous measurements, which are summarized in Fig. 2. We may list several reasons contributing to the difference:

1. The present measurements involve a large chamber, with many readout channels. The previous tests employed a single readout channel.
2. Ionization charges drifting from either side of the symmetrically placed anode plane are simultaneously recorded in the present tests. This saves space, but must cost something in resolution.
3. Residual errors remain, for the present data, after the baseline correction discussed above. The previous tests involved much shorter drift times ($\lesssim 400$ ns), and no such corrections were required.

The first, and probably also the second, of these points are endemic to a large chamber of practical geometry utilizing this technique. We believe that errors associated with baseline stability can, with modified readout electronics, be reduced to the level at which no off-line correction is required.

Conclusions

In our earlier work¹ and in new results by other groups presented at this conference^{5,6} one has seen the potential for significantly improving the resolving power of relativistic rise measurements by exploiting longitudinal drift and fast digitizing electronics to achieve very fine sampling of the ionization loss. This opens the possibility of compact and uncomplicated structures for particle detectors covering large solid angles in colliding beam experiments. In the work presented here we have investigated the fine sampling technique in a chamber of many readout channels, incorporating electrode structures readily amenable to the construction of a large detector which optimizes the ratio of fiducial track length to total detector length. We conclude that, in terms of the separation parameter defined in Fig. 2, a discrimination power corresponding to $S_{ep}(3.5 \text{ GeV/c}) \gtrsim 7$ is a realistic expectation for a

full scale detector of 1 meter fiducial length. This can be achieved with a detector whose total length is ~ 1.5 m. A conventional device, with 1-2 cm samples, would require ~ 3 m fiducial length to achieve the same sensitivity. (For the latter estimate we use the calculation of Allison & Cobb,² which has accurately predicted the performance of several large devices.)

We list here some of the issues which need further investigation before a full scale device can be feasibly undertaken:

- Stable control of the zero-signal level in the amplifier chain, as discussed above.
- Study of the response as a function of incident track angle; e.g. the sensitivity to local gain variations due to space charge effects.
- A systematic study of the momentum (velocity) dependence of the resolution.

In the meantime, a conceptual design for implementing such a detector in the environment of a high energy colliding beam experiment is given in Ref. 7.

Acknowledgments

We thank the staff of the CERN PS for assistance and technical support during the test beam runs, and we wish to acknowledge the excellent work of the technical staff of the CERN EF division in the design and construction of the test detector. We are indebted to R. Boie and V. Radeka of the BNL Instrumentation Division for assistance with the signal processing electronics. We thank Dr. A. Dwurazny for assisting with the data taking phase of this work.

This research supported in part by the U.S. Department of Energy under contracts DE-AC02-76CH00016 and DE-AC02-79ER10550.

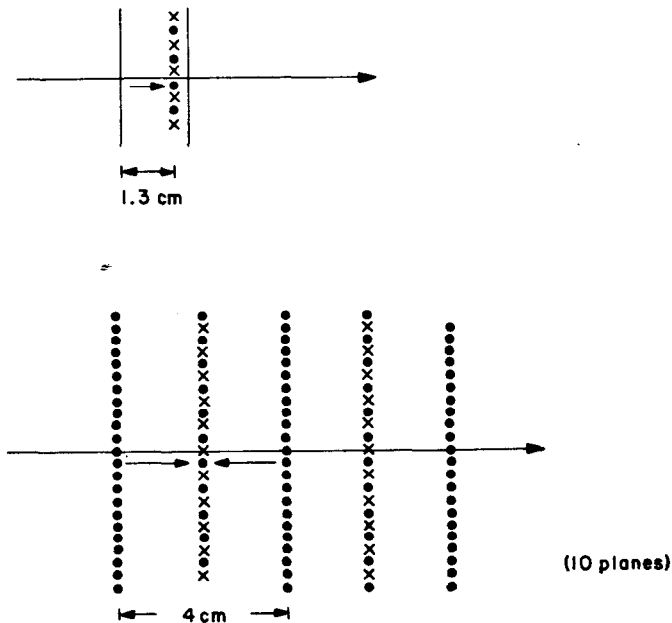


Fig. 1(a) Electrode geometry for the test chamber of Ref. 1. The long arrow represents a particle trajectory; the short arrow gives the direction of electron drift. The cathode planes are metal foils separated by 1.6 cm; (b) The geometry used for the tests reported here. The cathodes are wire planes. The full chamber consists of 10 active planes, of which 2 are shown here.

References

1. T. Ludlam *et al.*, IEEE Trans. Nucl. Sci., NS-28, 439 (1981).
2. W.W.M. Allison and J.H. Cobb, Ann. Rev. Nucl. Part. Sci., 30, 253 (1980).
3. R. Boie *et al.*, IEEE Trans. Nucl. Sci., NS-28, 603 (1981).
4. E. Platner, these proceedings.
5. F. Naito *et al.*, Univ. of Tokyo preprint INS-J-163 (1982) (Presented by T. Oshima at this Conf.)
6. R. Arai *et al.*, National Laboratory for High Energy Physics, Tsukuba preprint (1982) (Presented by Y. Watase at this Conf.)
7. T. Ludlam and E. Platner, Proc. 1981 ISABELLE Summer Workshop, BNL 51443, p. 1330 (1981).

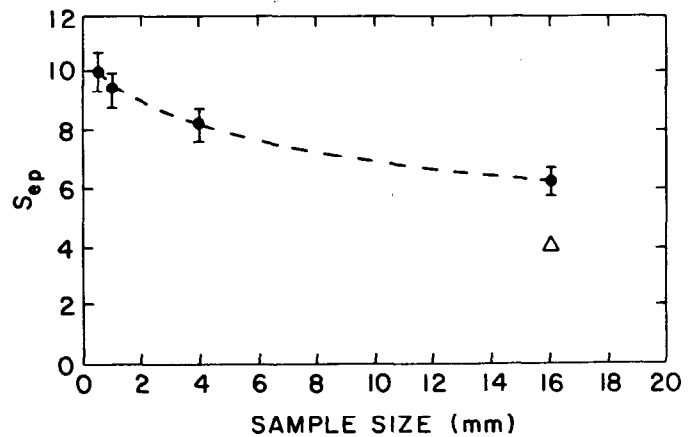
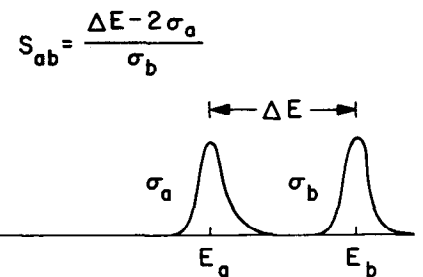


Fig. 2. The separation parameter S_{ab} is defined in the upper drawing, in terms of the difference ΔE between the centroids of the truncated mean distributions for particle types a and b, and the rms widths of the distributions. The lower plot summarizes the results from Ref. 1 for electrons and protons at 3.5 GeV/c, with 1 meter track lengths, as a function of the sample size. The open triangle gives the result from the ISIS-I detector (Ref. 2).

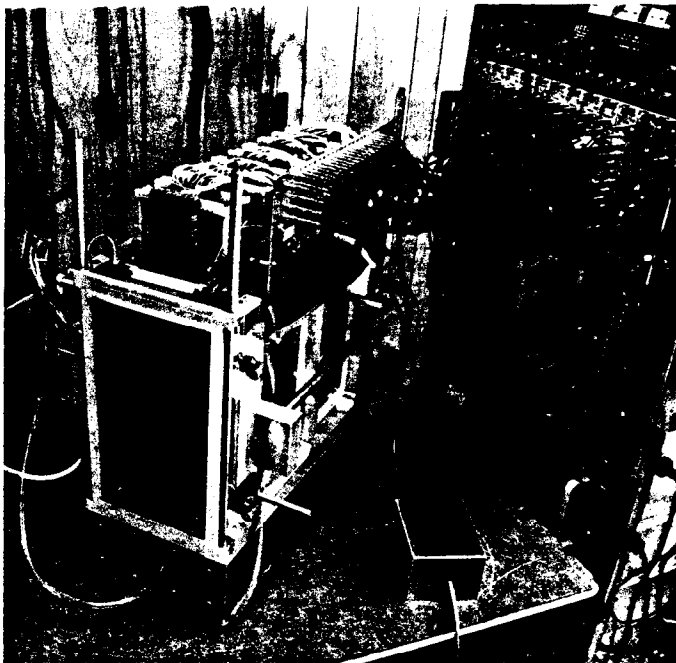


Fig. 3. The chamber just prior to insertion in the test beam. Direction of incidence is from the lower left. The wires are vertical, and the preamplifiers, seen at the top of the chamber, are attached directly to the ends of the anodes (there are 10 preamplifiers on each of 10 sense wire planes).

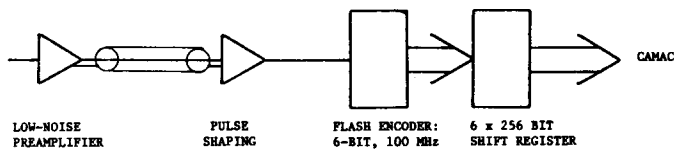


Fig. 4. The readout electronics chain.

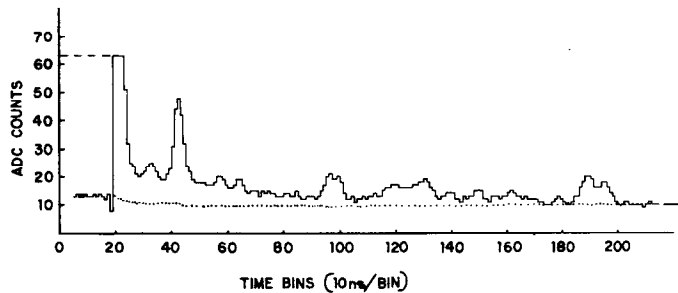


Fig. 5. The ADC response from a typical track through one cell (4 cm) of the chamber. Full range of the ADC is 64 counts on the vertical scale. The dotted curve under the signal gives the computed baseline for this event (see text).

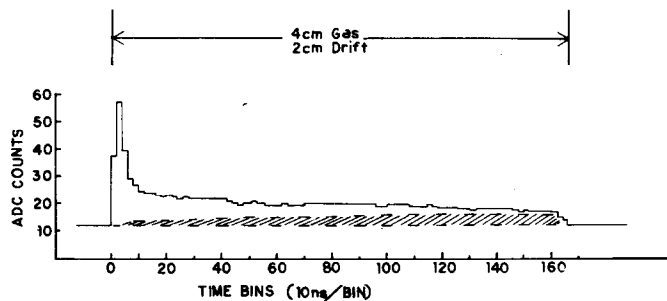


Fig. 6. The ADC response averaged over many (proton) tracks, after baseline correction. The shaded area falls below the baseline in the uncorrected data.

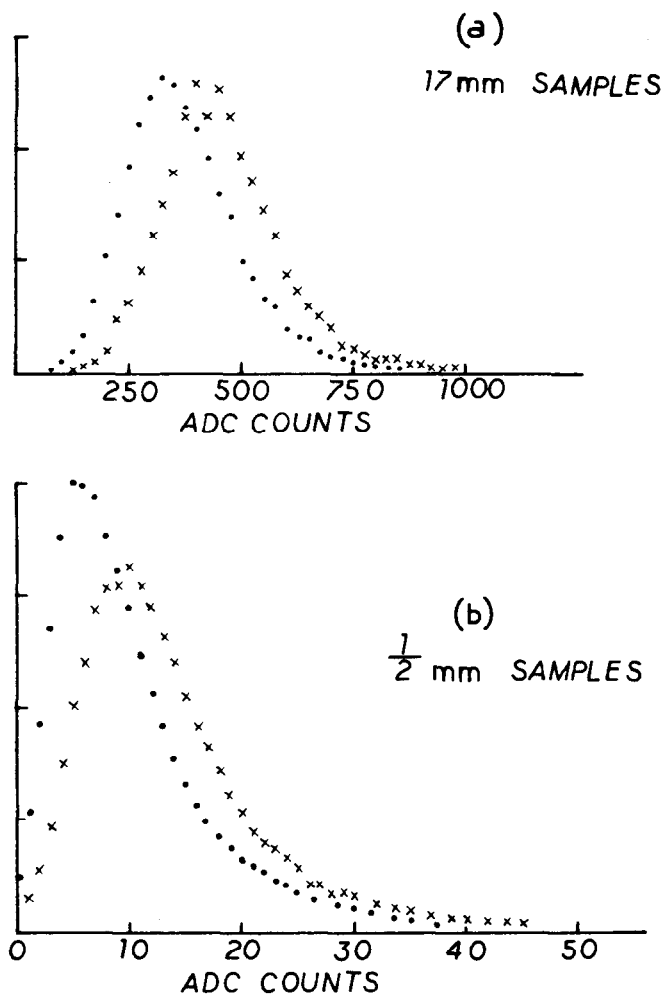


Fig. 7. Pulse height spectra for protons (dots) and electrons (x's). (a) 17 mm samples (64 time bins per sample); (b) $\frac{1}{2}$ mm samples (2 time bins per sample). Electrons and protons are normalized to the same area in each plot.

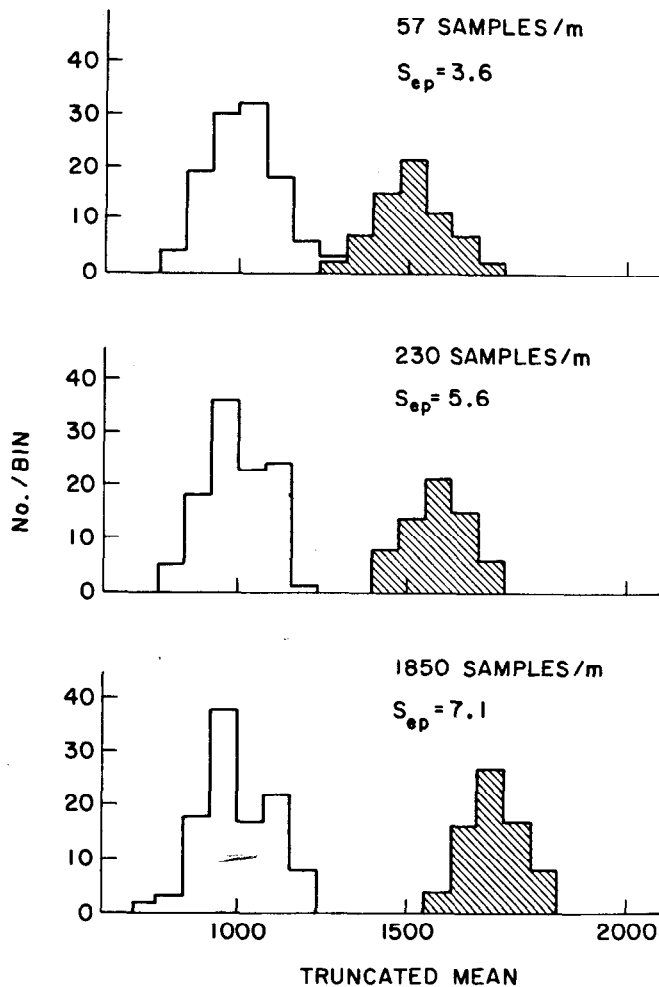


Fig. 8. The truncated means for 110 proton tracks (open histogram) and 72 electron tracks (shaded). Each track is 1 meter long. The results are shown for 3 different sample sizes.